Theory of the Magnetic Properties of the Ilmenites $MTiO_3$

JOHN B. GOODENOUGH AND JOHN J. STICKLER
Lincoln Laboratory, Massachusetts Institute of Technology, Lexington, Massachusetts*
(Received 7 June 1967)

Crystal-field, superexchange, and molecular-field theories have been used to analyze available experimental data for the ilmenites $MnTiO_3$, $FeTiO_3$, $CoTiO_3$, and $NiTiO_3$. The magnetic order and spin directions are shown to be compatible with negative trigonal fields in all compounds. Crystallographic considerations indicate that $FeTiO_3$ has its negative trigonal field enhanced by spin-orbit coupling and by a large magnetic anisotropy orienting spins along the c_h axis, even in the paramagnetic region. This invalidates the interpretation of the paramagnetic susceptibility of $FeTiO_3$ by an isotropic model. $MnTiO_3$ exhibits three anomalies: a reduced atomic moment (4.55 μ_B) in the magnetically ordered state, a broad maximum in χ_m versus T above T_N, and a discrepancy in the molecular-field exchange parameters obtained from high-temperature susceptibilities and low-temperature resonance with only dipole-dipole magnetic anisotropy. A similar but smaller discrepancy in exchange parameters was also found for $NiTiO_3$. These difficulties disappear if exciton transfer between superexchange-coupled cations is introduced. This is a correlated superexchange involving the simultaneous transfer of electrons on neighboring cations to one another. For Mn^{2+} ions coupled antiferromagnetically via 90° cation-anion-cation superexchange, this exciton superexchange induces not only ^4T excited Mn^{2+} states, but also ^2T excited states via a double-exciton transfer. This introduces a large reduction in moment below T_N, an increase in moment with temperature through the range of short-range order above T_N, and an additional anisotropy. The latter has the sign required to reconcile susceptibility and resonance data provided that the ^2T excited state is more populated than the ^4T states. The same mechanism for $CoTiO_3$ and $NiTiO_3$ does not change the atomic moments and gives the correct sign for the additional anisotropy. The data are consistent with a magnetostriction below T_N in $CoTiO_3$ that reduces the trigonal component of the crystalline field to nearly zero.

I. INTRODUCTION

MAGNETIC-SUSCEPTIBILITY, magnetic-resonance, neutron-diffraction, specific-heat, and x-ray diffraction data are now available for the antiferromagnetic ilmenites $MTiO_3$, where M=Mn, Fe, Co, and Ni. These provide an opportunity to check the adequacy of crystal-field, superexchange, and molecular-field theories for these layer compounds. It is shown that the data for $MnTiO_3$ cannot be adequately handled by these theories, but can be accounted for within this framework if an exciton-exchange mechanism is present. Some independent evidence for this latter mechanism in other compounds containing magnetically ordered Mn^{2+} ions is also cited.

II. STRUCTURE

The corundum (Al_2O_3) structure consists of a close-packed-hexagonal anion sublattice that has $\frac{2}{3}$ of its octahedral sites occupied by cations. The octahedral sites form a simple-hexagonal array and share common faces along the hexagonal c_h axis, common edges within the hexagonal basal planes. The $\frac{1}{3}$ octahedral-site vacancies are ordered so as to minimize the cation-sublattice electrostatic repulsive forces: Each cation has only one near-neighbor cation along c_h and three near-neighbor cations within the basal planes. Electrostatic forces between cationic pairs along c_h displace the cations from the centers of symmetry of their anionic interstices, so that the basal-plane layers of cations and anions are puckered.

The ilmenite structure is an ordered corundum structure in which the Ti^{4+} and M^{2+} ions occupy alternate basal-plane layers of cationic sites. The cationic sublattice is shown in Fig. 1, where the rhombohedral, primitive unit cell is also indicated. The size of this cell is the same as that of the corundum structure, even though there is ordering of unlike cations on alternate (111) cationic planes to give the octahedral-site sequence along c_h:

$$—\square—Ti^{4+}—M^{2+}—\square—M^{2+}—Ti^{4+}—\square—,$$

where $\square$ symbolizes a vacancy. The puckering induced by electrostatic M^{2+}–Ti^{4+} repulsions is also indicated in Fig. 1. This makes the Ti^{4+}–M^{2+} separation per rhombohedral c_R

$$s=u-v, \tag{1}$$

where $\pm(u, u, u)$ and $\pm(v, v, v)$ are the crystallographic parameters in $R\bar{3}$ symmetry for the M^{2+} and Ti^{4+} positions. Figure 2 shows a plot of s versus the number of $3d$ electrons per M^{2+} ion, and it is apparent that there is an anomalously large separation in $FeTiO_3$. The magnitude of the cationic displacements per cell length c_R is

$$\tfrac{1}{2}(s-s_0)=\tfrac{1}{2}\{(u-v)-0.167\}. \tag{2}$$

This gives a measure of the magnitude of the cationic puckering.

III. CRYSTAL-FIELD THEORY

The ilmenites studied are antiferromagnetic insulators having a large electronegativity difference between cations and anions. This indicates that the cationic $3d$ electrons occupy *localized* orbitals having energies within a large (5–10 eV) energy gap between the valence-band (mostly anionic $2s$, $2p$ in character) energies and the

* Operated with support from the U.S. Air Force.

conduction-band (mostly cationic $4s$, $4p$ in character) energies. Therefore *crystal-field theory* is appropriate for the phenomenological description of one-ion d-electron energies and *superexchange theory* for interatomic spin correlations.

The localized-d-electron Hamiltonian has the form

$$\mathcal{H}=\mathcal{H}_0+V_{el}+V_c+(V_{LS}+V_T)+\mathcal{H}_{ex}+\mathcal{H}_D+\mathcal{H}_z, \quad (3)$$

where $\mathcal{H}_0$ is the energy of a single, localized electron moving in the spherical potential of its atomic nucleus and all the other electrons. Its solutions give hydrogenic wave functions with angular dependencies

$$f_0\sim r^{-2}\{(z^2-x^2)+(z^2-y^2)\}=3\cos^2\theta-1, \quad (4)$$

$$f_{\pm1}\sim r^{-2}\{yz\pm izx\}=\sin\theta\cos\theta\exp(\pm i\phi), \quad (5)$$

$$f_{\pm2}\sim 2r^{-2}\{(x^2-y^2)\pm ixy\}=\sin^2\theta\exp(\pm i2\phi). \quad (6)$$

Two corrections to the spherical potential must be made: $V_{el}+(V_c+V_T)$. The first, which is present if there are more than one outer electron and hole in the d shell, is an intra-atomic correlation energy. It is responsible for Hund's highest-multiplicity rules for the free ion. The second is the crystal-field energy. In the ilmenite structure it contains a cubic component V_c and a smaller trigonal component V_T. These fields include covalent mixing of the atomic d orbitals with the anionic $2s$ and $2p$ orbitals. This covalent mixing does not change the symmetry of the atomic orbitals derived from a point-charge model, but it does increase the radial extension of the localized wave functions. In the ilmenites $(V_c+V_T)<V_{el}$, so that the M^{2+} ions are all in the high-spin state, which gives the free-ion and cubic-field ground-state terms shown in Table I. The cubic-field splittings are summarized in Figs. 3 and 4. (There is no splitting of the ^6S term.) Note

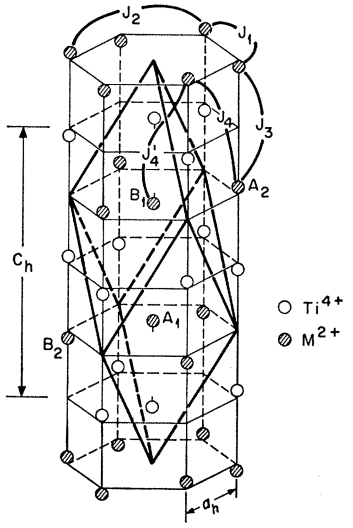

FIG. 1. Cation sublattice of the ilmenite structure showing primitive, rhombohedral unit cell, hexagonal lattice parameters, and the five principal superexchange interactions J_1, J_2, J_3, J_4, and J_4'.

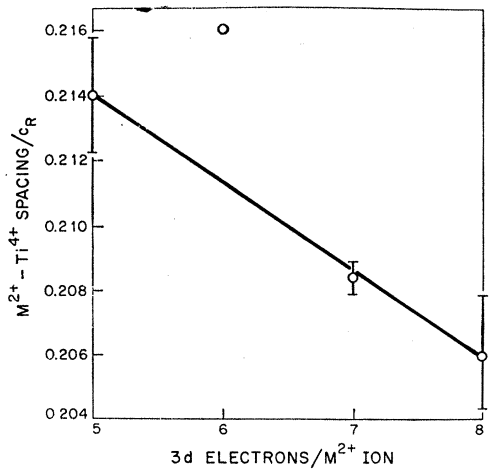

FIG. 2. M^{2+}—Ti^{4+} separation per rhombohedral c_R axis versus the number of outer $3d$ electrons per M^{2+} ion.

that the ^3F state corresponds to two d holes, so that the splitting is the inverse of that for the two d electrons outside a closed half-shell in the ^4F state.

The T_{2g} and T_{1g} terms each contain a threefold orbital degeneracy having azimuthal orbital momenta $M_L=0,\ \pm1$. (The cubic fields split $f_{\pm2}$ into two real components, thereby quenching $L_z=i\hbar\partial/\partial\varphi$ for $M_L=\pm2$.) These threefold orbital degeneracies are split by the combined perturbation

$$V_{LS}+V_T+\mathcal{H}_{ex}=ak_c\lambda\mathbf{L}\cdot\mathbf{S}+\delta(L_z^2-\tfrac{2}{3})-2J_p\langle S\rangle S_z, \quad (7)$$

where λ is the atomic spin-orbit-coupling parameter and k_c is a large fraction that is determined empirically from paramagnetic-resonance experiments. It contains the reduction in effective λ due to covalent mixing[1] and, in the case of Co^{2+}, the mixing of $^4T_{1g}(^4F)$ and $^4T_{1g}(^4P)$ terms.[2] The parameter a expresses the isomorphism between $L=2$ states of T_{2g} or T_{1g} and $L=1$ states of P symmetry:

$$a=-1 \quad \text{for } Fe^{2+} \text{ ions}, \quad (8)$$

$$a=-\tfrac{3}{2} \quad \text{for } Co^{2+} \text{ ions}. \quad (9)$$

The trigonal component of the crystalline fields V_T splits the $M_L=0$ and $M_L=\pm1$ states by the energy δ, and the expression in Eq. (7) rests on the assumption that for small δ the energy of the T_{2g} or T_{1g} manifold is conserved. Here z is the crystalline trigonal axis and δ may be either positive or negative. In the molecular-field approximation,

$$\mathcal{H}_{ex}=-\sum_{ij}J_{ij}\mathbf{S}_i\cdot\mathbf{S}_j\approx-2J_p\langle S\rangle S_{z'}, \quad (10)$$

where J_p is the net near-neighbor exchange parameter defined by Eq. (30) and Table II and z' is the spin axis in the magnetically ordered state. The coefficients

[1] M. Tinkham, Proc. Roy. Soc. (London) **A236**, 549 (1956).
[2] J. Kanamori, Progr. Theoret. Phys. (Kyoto) **17**, 177 (1957); **17**, 197 (1957).

TABLE I. Free-ion and cubic-field ground-state terms for M^{2+} ions in $MTiO_3$, low-temperature ($T<T_N$) ground states $|M_L, M_S\rangle$ in first-order perturbation ($V_{LS}+V_T+\mathcal{H}_{ex}$), g factors from Zeeman splittings, and isotropic corrections Δ_g from second-order perturbations V_{LS}.

Ion	V_{el}	V_c	$V_{LS}+V_T+\mathcal{H}_{ex}$	$\mathcal{H}_Z$	Δg[a]
Mn^{2+}	^6S	$^6A_{1g}$	$\|0, 5/2\rangle$	$g_{\|\|}=g_\perp=2.0$	≈ 0
Fe^{2+}	^5D	$^5T_{2g}$	$a_1\|-1, 2\rangle+a_2\|0, 1\rangle+a_3\|1, 0\rangle$[b]	$g_{\|\|}=2\{(k_c+4)a_1^2+2a_2^2-k_c a_3^2\}$, $g_\perp=0$	
Co^{2+}	^4F	$^4T_{1g}$	$b_1\|-1, \frac{3}{2}\rangle+b_2\|0, \frac{1}{2}\rangle+b_3\|1, -\frac{1}{2}\rangle$	$g_{\|\|}=(3k_c+6)b_1^2+2b_2^2-(3k_c+2)b_3^2$ $g_\perp=4b_2^2+4\sqrt{3}b_1b_3-3\sqrt{2}k_c b_2 b_3$	$(15/2)\|\lambda\|k_c^2/\Delta$
Ni^{2+}	^3F	$^3A_{2g}$	$\|0, 1\rangle$	$g_{\|\|}=g_\perp=2.0$	$8\|\lambda\|k_c^2/\Delta'$

[a] $\Delta=E(T_{2g})-E(T_{1g})$; $\Delta'=E(T_{2g})-E(A_{2g})$. [b] For a negative trigonal field ($\delta_{Fe}<0$).

a_1, a_2, a_3 and b_1, b_2, b_3 of Table I are obtained from the secular equations of Eq. (7) for the ground-state energy. This secular determinant factors into separate equations for different M_J, as illustrated schematically for $\mathcal{H}_{ex}=0$ in Figs. 5 and 6. In a magnetically ordered state, $\mathcal{H}_{ex}$ provides a molecular field that splits any Kramers doublets and increases the magnitude of the ground-state atomic moments. Note that for $\delta=0$ and $\mathcal{H}_{ex}=0$, V_{LS} splits the cubic-field terms into levels with different J, each having the degeneracy $(2J+1)$ and separated by the Landé interval rule

$$E_J-E_{J-1}=ak_c\lambda J. \tag{11}$$

If $V_{LS}=0$ and $\mathcal{H}_{ex}=0$, on the other hand, V_T splits the terms into states of different M_L.

The dipole-dipole interaction energy $\mathcal{H}_D$ introduces a magnetic anisotropy, and Zeeman splittings in an internal magnetic field H_i define the spectroscopic splitting tensor $\mathbf{g}$ via the relation

$$\mu_B\mathbf{H}_i\cdot\mathbf{g}\cdot\mathbf{S}'=\langle\Psi\,|\,\mathcal{H}_z\,|\,\Psi\rangle=\mu_B\mathbf{H}_i\cdot\langle\Psi\,|\,ak_c\mathbf{L}+2\mathbf{S}\,|\,\Psi\rangle, \tag{12}$$

where S' is the effective spin of the ground state. In general, Eq. (12) gives a $g_{||}\neq g_\perp$ wherever $\delta\neq 0$ and the cubic-field term is T_{2g} or T_{1g}. This anisotropy introduces an anisotropy energy K_g, which must be added to the dipole-dipole anisotropy K_D, as discussed in Sec. VI.

Finally, spin-orbit coupling introduces matrix elements between the ground state and higher terms to give a second-order correction to the spectroscopic splitting factor of the form

$$\Delta g=\sum_n c_n\,|\,\lambda\,|\,k_c^2/\Delta_n, \tag{13}$$

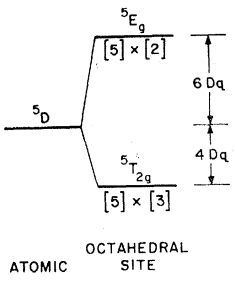

FIG. 3. Cubic-field splitting of a ^5D electronic level on an octahedral-site cation. Conservation of energy of the ^5D manifold occurs only in a point-charge model. Covalent mixing enhances the splitting $10D_q$ and destroys the energy conservation. Numbers in brackets refer to spin and orbital degeneracies.

where Δ_n is the splitting of the higher term from the ground state.

IV. MOLECULAR-FIELD THEORY

A. Mn^{2+} and Ni^{2+}

1. Magnetic Susceptibility

Where the ground state is separated from the next higher state by an energy large compared to kT, as in $MnTiO_3$ and $NiTiO_3$, the molecular-field equations, given an applied field H_0, are

$$M_iT-C_i[H_0+\sum_{ij}\Lambda_{ij}M_i]=0, \tag{14}$$

$$\mathbf{M}=\sum_i\mathbf{M}_j. \tag{15}$$

The indices i and j refer to the magnetic sublattice. If there is a negligible crystal-field anisotropy, as in $MnTiO_3$ and $NiTiO_3$, the Weiss-field constants Λ_{ij} for a two-sublattice model are related to the exchange parameters J_{ij} of Eq. (10) via

$$\mathcal{H}_{ex}=-\sum_i\mathfrak{y}_i\cdot\mathbf{H}_{Wi}$$

$$=-\sum_{ij}\Lambda_{ij}\tfrac{1}{2}N\mathfrak{y}_i\cdot\langle\mathfrak{y}_j\rangle\approx\sum_{ij}J_{ij}\mathbf{S}_i\cdot\mathbf{S}_j \tag{16}$$

and

$$\Lambda_{ij}=2J_{ij}/k\tau, \qquad k\tau\equiv Ng^2\mu_B^2. \tag{17}$$

Elimination of the M_i from Eqs. (14) and (15) gives the Curie-Weiss law

$$\chi_m=C_m/(T-\Theta_p); \qquad C_m=\tfrac{1}{3}\tau S(S+1), \tag{18}$$

where

$$\Theta_p=\tfrac{1}{2}C_m(\Lambda_{++}+\Lambda_{+-}) \tag{19}$$

and Λ_{++}, Λ_{+-} are the net intrasublattice and intersublattice Weiss-field constants for the two-sublattice array. The Néel temperature is the largest real root of the secular equation for the M_i, Eq. (14), with $H_0=0$;

$$T_N=\tfrac{1}{2}C_m(\Lambda_{++}-\Lambda_{+-}). \tag{20}$$

Further, substitution of Eqs. (19) and (20) into Eq.

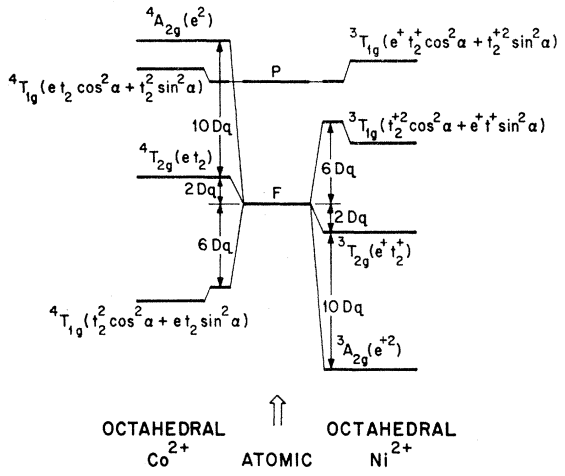

FIG. 4. Cubic-field splitting of two-electron (Co^{2+}) and two-hole (Ni^{2+}) F and P levels. Conservation of energy holds only in a point-charge model.

(18) gives

$$\chi_m(T_N) = -1/\Lambda_{+-}. \tag{21}$$

Thus Eqs. (17)–(21) permit expression of the exchange parameters, in °K, in terms of the observables Θ_p, T_N, C_m, and $\chi_m(T_N)$;

$$2J_{++}/k = (\Theta_p + T_N)(\tau/C_m), \tag{22}$$

$$2J_{+-}/k = (\Theta_p - T_N)(\tau/C_m) = -\tau/\chi_m(T_N). \tag{23}$$

Because the molecular-field approximation neglects short-range order in the vicinity of T_N, these expressions are not quantitative and $\chi_m(T_N)$ gives an upper bound to the exchange parameter J_{+-}.

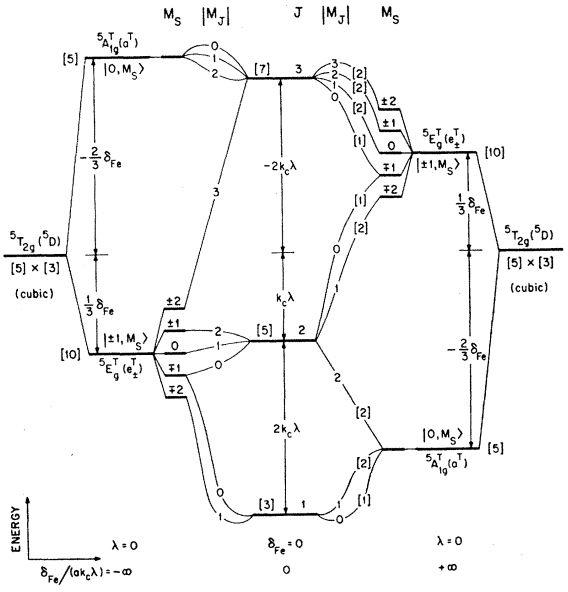

FIG. 5. Schematic spin-orbit plus trigonal-field splittings of cubic-field ${}^5T_{2g}$ level of Fe^{2+} as a function of the ratio $\delta_{Fe}/(ak_c\lambda)$. Positive ratios correspond to positive axial fields.

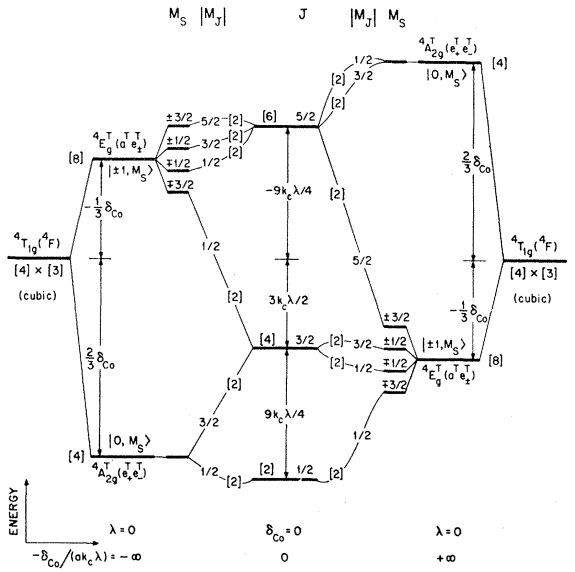

FIG. 6. Schematic spin-orbit plus trigonal-field splittings of cubic-field ${}^4T_{1g}$ level of Co^{2+} as a function of the ratio $-\delta_{Co}/(ak_c\lambda)$, where positive ratios correspond to positive axial fields.

2. *Antiferromagnetic Resonance*

For a simple two-sublattice, collinear-spin configuration in zero external field, the antiferromagnetic-resonant frequency is

$$\omega_R \approx \gamma\{H_A^2 + 2H_AH_E\}^{1/2} \approx \gamma(-2\Lambda_{+-}|K|)^{1/2}, \tag{24}$$

where $\gamma \equiv ge/2mc$, $H_A \equiv |K|/M_i$, and $H_E \equiv -\Lambda_{+-}M_i$. Here K is the anisotropy constant. If K is known, this provides an independent check of the parameter J_{+-} in the low-temperature ($T < T_N$) interval;

$$2J_{+-}/k = -\omega_R^2\tau/(2\gamma^2|K|) = -\hbar^2\omega_R^2 N/(2k|K|). \tag{25}$$

B. Fe^{2+} and Co^{2+}

Where the ground state is separated from the next higher state by an energy comparable to kT, the magnetic susceptibility must be obtained from the statistical mean over all the populated states Ψ_i of energy E_i,

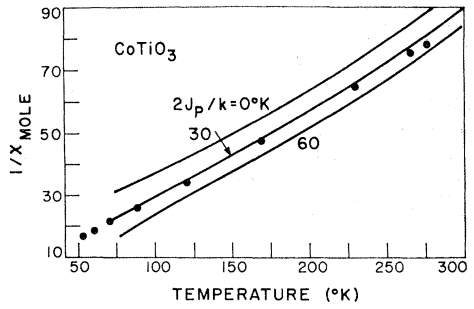

FIG. 7. Inverse susceptibility versus temperature for $CoTiO_3$ for three different values of the parameter $2J_p/k$. Experimental points are from Ref. 2.

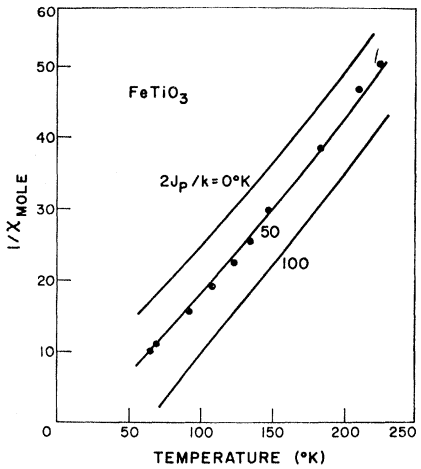

FIG. 8. Inverse susceptibility versus temperature for $FeTiO_3$ for three different values of the parameter $2J_p/k$. Experimental points are from Ref. 2.

weighted by the Boltzmann factor, and

$$\chi_m=(N/H_0)\sum_i \mu_i \exp(-\beta E_i)/\sum_i \exp(-\beta E_i), \quad (26)$$

where $\beta\equiv 1/kT$. To second order in the applied field,

$$E_i=E_i^{(0)}+\langle i \mid \mathcal{H}_{ex}+\mathcal{H}_z \mid i\rangle + \sum_j{}' \langle j \mid \mathcal{H}_{ex}+\mathcal{H}_z \mid i\rangle^2/(E_i^{(0)}-E_j^{(0)}), \quad (27)$$

where $E_i^{(0)}$ is the solution of the field-independent problem, including $V_{LS}+V_T$. For a given ratio $\delta/ak_c\lambda$, these energies are obtained directly from the secular equation. In the molecular-field approximation and with $\delta\approx 0$, it follows from Eqs. (10) and (12) that $\mathcal{H}_{ex}+\mathcal{H}_z$ is proportional to H_0, since for $T>T_N$ and $\delta=0$ the average spin $\langle S\rangle$ is proportional to the field H_0 that induces it. This gives

$$E_i=E_i^{(0)}+E_i^{(1)}H_0+E_i^{(2)}H_0^2+\cdots, \quad (28)$$

where $E_i^{(1)}$ and $E_i^{(2)}$ are obtained from Eq. (27) and the Ψ_i, Ψ_j obtained from the secular equations for the $E_i^{(0)}$. Kanamori[2] has derived expressions for these energies for octahedral site Fe^{2+} and Co^{2+}. Since $\mu_i=-\partial E_i/\partial H_0$, the susceptibility to zero order in H_0 is

$$\chi_m=\frac{N\sum_i[\beta(E_i^{(1)})^2-2E_i^{(2)}]\exp(-\beta E_i^{(0)})}{\sum_i \exp(-\beta E_i^{(0)})}. \quad (29)$$

In order to calculate χ_m versus T from this expression, it is necessary to first obtain a self-consistent expression for $\langle S\rangle$. The result is a complicated function of T, which is shown graphically in Figs. 7 and 8 for several values of the parameter

$$J_p\equiv J_{++}+J_{+-}. \quad (30)$$

To obtain an expression corresponding to Eq. (20), Kanamori has made use of the fact that an infinitesimal antiferromagnetic exchange field H_E sets in at T_N, since the magnetic transition is second order. He obtained the expression

$$2J_N=\sum_{J,M} A/\sum_{J,M} A\{\beta_N\langle J, M \mid S_{z'}{}^2 \mid J, M\rangle + 2\sum_J{}' \langle J, M \mid S_{z'} \mid J', M\rangle^2/\Delta_{JJ'}\}, \quad (31)$$

where

$$J_N\equiv J_{++}-J_{+-}, \quad A\equiv\exp(-\beta_N E_J^{(0)}), \quad \beta_N\equiv 1/kT_N, \quad \Delta_{JJ'}\equiv E_J-E_{J'}, \quad (32)$$

and z' defines the spin direction.

V. SUPEREXCHANGE

In the ilmenite structure, there are the five superexchange interactions shown in Fig. 1 and labeled by the *magnitudes* J_1, J_2, J_3, J_4, and J_4'. According to the general rules for superexchange coupling,[3] the signs of the superexchange interactions depend upon the occupancies of the interacting orbitals: If there is one electron per interacting orbital, the exchange parameter is negative, corresponding to antiferromagnetic coupling; if there is more than one electron per interacting orbital, the exchange parameter is positive.

The crystalline fields split the one-electron orbitals $\mid M_L, M_s\rangle$ of Eqs. (4)–(6) into the orbitals

$$e_1\sim 3\cos^2\theta_0-1 \quad \text{and} \quad e_2\sim\sin^2\theta_0\cos 2\phi_0, \quad (33)$$

$$\mid 0, M_s\rangle\equiv a^T\sim 3\cos^2\theta_T-1, \quad (34)$$

$$\mid \pm 1, M_s\rangle\equiv e_\pm{}^T\sim c_1\sqrt{2}\sin^2\theta_T\exp(\mp i2\phi_T) \pm c_2\sin\theta_T\cos\theta_T\exp(\pm i\phi_T), \quad (35)$$

where $\theta_T=0$ is the c_h axis and $\phi_T=0$ is an a_h axis defined as shown in Fig. 1. The angles θ_0 and ϕ_0 are referred to cation-oxygen bonds. In cubic symmetry, $c_1=c_2$. In a trigonal field, orbitals e_1 and e_2 mix with $e_\pm{}^T$ to make $c_1\neq c_2$ and alter the form of e_1 and e_2. Each of the M^{2+} cations of this study has one e_1 and one e_2 electron, so that interactions via these orbitals (to be referred to as e orbitals) are antiferromagnetic. Mn^{2+} also has one electron per a^T and $e_\pm{}^T$ orbital, whereas the other cations (Fe^{2+}, Co^{2+}, Ni^{2+}) have more than one electron in each of these orbitals. (These will be referred to hereafter as t orbitals.) In Ni^{2+} they are filled and, from Table I, each is more than half-filled in Fe^{2+} and Co^{2+} so long as none of the coefficients a_i or b_i vanishes. Therefore, interactions via t orbitals or via a t orbital on one cation and an e orbital on the other are antiferromagnetic in $MnTiO_3$, but ferromagnetic in $FeTiO_3$, $CoTiO_3$, and $NiTiO_3$.

The interaction J_1 contains two contributions: a cation-cation interaction via the direct overlap of t orbitals of neighboring cations and a 90° cation-anion-cation interaction. The latter is dominated by the cou-

[3] J. B. Goodenough, *Magnetism and the Chemical Bond* (John Wiley & Sons, Inc., New York, 1963). W. P. Osmond [Brit. J. Appl. Phys. **15**, 1377 (1964)] discusses the ilmenites specifically.

TABLE II. Predicted signs of the exchange parameters and magnetic order for the ilmenites MTiO$_3$.

Compound	Magnetic order	J_{++}	J_{+-}
MnTiO$_3$	A_1A_2 anti B_1B_2, S $\|\|$ c_h (A_1B_1 anti A_2B_2 if $6J_4>J_3+3J_4'$)	$-6J_2-6J_4$	$-3J_1-J_3-3J_4'$
FeTiO$_3$	A_1B_2 anti A_2B_1, S $\|\|$ c_h	$3J_1-6J_2$	$-J_3-6J_4-6J_4'$
CoTiO$_3$	A_1B_2 anti A_2B_1, S$\perp c_h$	$3J_1-6J_2$	$-J_3-6J_4-6J_4'$
NiTiO$_3$	A_1B_2 anti A_2B_1, S$\perp c_h$	$3J_1-6J_2$	$-J_3-6J_4-6J_4'$

pling of a t orbital on one cation with an e orbital on the other. Since the e orbitals are half-filled in all ions and the t orbitals are half-filled in Mn^{2+}, but more than half-filled in Fe^{2+}, Co^{2+}, and Ni^{2+}, it follows from the superexchange rules that

$$J_1^{Mn}<0 \quad \text{and} \quad J_1^{Fe}>0, \qquad J_1^{Co}>0, \qquad J_1^{Ni}>0. \tag{36}$$

The other interactions are all cation-anion-anion-cation interactions. With two anion intermediaries, they are relatively weak. Cation-anion σ bonding, which involves the e orbitals, dominates the interactions J_2, J_4, and J_4'. Since the e orbitals each contain only one electron, these interactions are expected to be antiferromagnetic and weak relative to J_1 in all compounds. The interaction J_3 also contains an overlap of a^T orbitals directed along c_h. In Mn^{2+} it is antiferromagnetic, so that the net magnitude J_3 is intermediate between J_1 and the other parameters. In the other compounds the a^T-orbital overlap gives a positive contribution to J_3, so that it has a small net magnitude. In terms of the sublattices A_1, A_2, B_1, and B_2 in Fig. 1, this reasoning leads to the predictions of Table II for the magnetic order below T_N. The spin directions given in this table depend upon the sign of the magnetic anisotropy constant $K=K_D+K_g$, where K_D is calculated below and shown in Table III and it is assumed that only in F_0TiO_3 the sign of K is determined by K_g.

VI. ANISOTROPY

A. Dipole-Dipole Interactions

Magnetic dipole energies have the form

$$\mathcal{H}_D=(1/8)N^2\mu^2\sum_{s=1}^{4}\Phi_s, \tag{37}$$

where the Φ_s are dipole sums, to be carried out within a Lorentz sphere, for each sublattice s;

$$\Phi_s=4/N\sum_j[1-3\cos^2(c_h, r_{ij})]r_{ij}^{-3}. \tag{38}$$

$4/N$ is the number of magnetic cations per cm^3 in a sublattice and j runs over all cations of a sublattice s. It is convenient to define

$$\Phi^c=\sum_s\Phi_s \quad \text{and} \quad \Phi^a=\sum_s\Phi_s^a, \tag{39}$$

where Φ^c and Φ^a are the dipole sums for spins parallel and perpendicular to c_h. Then the dipole-dipole anisotropy at $T=0$°K is

$$K_D=(1/8)N^2\mu^2(\Phi^c-\Phi^a), \tag{40}$$

where

$$\Phi=\Phi_{A1}-\Phi_{B1}\pm\Phi_{A2}\mp\Phi_{B2}, \tag{41}$$

in accordance with the order given in Table II. The computed sums Φ^c, Φ^a and anisotropy energy K_D are displayed in Table III. The magnitudes of the atomic moments are taken from Eqs. (42), (48), and (51).

B. Anisotropic g Factors

1. Mn^{2+} and Ni^{2+}

From Table I, the Mn^{2+} and Ni^{2+} ions have isotropic g factors, so that $K_g=0$ and

$$\mu^{Mn}=gS\mu_B=5\mu_B, \qquad \mu^{Ni}=(g+\Delta g)S\mu_B=2.22\mu_B. \tag{42}$$

2. Fe^{2+}

From Fig. 5, the ground state of the Fe^{2+} ion in $FeTiO_3$, given a negative trigonal field ($\delta_{Fe}<0$), is a doublet having effective spin $S'=\frac{1}{2}$. Such a state has the highly anisotropic g factor shown in Table I. If $\delta_{Fe}=0$, on the other hand, the ground state is a triplet ($S'=1$) and the additional ground-state wave func-

TABLE III. Atomic moments $\mu=n_A\mu_B$, dipole-dipole sums, and anisotropy energies in erg/cm^3 for several ilmenites.

Compound	n_A (theoret)	n_A (expt)	$\Phi^c\times10^{-24}$	$\Phi^a\times10^{-24}$	$K_D\times10^{-6}$
MnTiO$_3$	5	4.55	0.0270	0.0540	-1.6[a]
FeTiO$_3$	4.2	>4.0	0.2357	0.1179	+5.2
CoTiO$_3$	2.5		0.2455	0.1227	+1.9
NiTiO$_3$	2.22	2.25	0.2456	0.1273	+1.6

[a] If $\mu^{Mn}=4.55\mu_B$, then $K_D=-1.36\times10^6$ erg/cm^3.

tion is

$$\Psi_0 = a_1' \mid -1, 1\rangle + a_2' \mid 0, 0\rangle + a_1' \mid 1, -1\rangle. \quad (43)$$

This leaves $g_{||}$ of Table I unchanged, but makes

$$g_\perp = -k_c(a_1'a_2 + a_2'a_3) + 2\sqrt{2}a_1'a_1 + 2\sqrt{3}(a_2'a_2 + a_1'a_3). \quad (44)$$

In the limit $\mathcal{H}_{ex}=0$, solution of the secular equation for $M_J=1$ and 0 gives, to first order in δ/λ,

$$a_1 = \{\tfrac{3}{5} + 0.23\delta/3k_c\lambda\}^{1/2}, \qquad a_2 = -\{\tfrac{3}{10} - 0.20\delta/3k_c\lambda\}^{1/2},$$
$$a_3 = \{\tfrac{1}{10} - 0.03\delta/3k_c\lambda\}^{1/2},$$
$$a_1' = \{\tfrac{3}{10} + 0.144\delta/3k_c\lambda\}^{1/2},$$
$$a_2' = -\{\tfrac{2}{5} - 0.288\delta/3k_c\lambda\}^{1/2}. \quad (45)$$

Since $S'=1$, it follows that

$$g_{||} = (3 + \tfrac{1}{2}k_c) + 0.52(1 + \tfrac{1}{2}k_c)\,\delta/3k_c\lambda,$$
$$g_\perp = (3 + \tfrac{1}{2}k_c) - 0.26(1 + \tfrac{1}{2}k_c)\,\delta/3k_c\lambda. \quad (46)$$

Below the Néel temperature T_N, the spins are all collinear and the energy $\mathcal{H}_{ex}$ is optimized by the state with a maximum g factor parallel to the Weiss molecular field. This occurs for spins parallel to the trigonal axis and $\delta/\lambda>0$, or $\delta_{Fe}<0$. Therefore, in the absence of a dipole-dipole energy and a $\delta_{Fe}=0$ in the paramagnetic state, there is a spontaneous crystallographic change below T_N to make $\delta_{Fe}<0$ and $K_g<0$. In fact, however, there is a dipole-dipole energy $K_D>0$, so that such a crystal-field stabilization is done at the expense of K_D. Nevertheless, the magnetic order and spontaneous crystallographic distortion below T_N in FeO indicate that if $\delta_{Fe}\leq 0$ above T_N, then K_D is not large enough to quench a spontaneous increase in the Fe^{2+}–Ti^{4+} separation that makes $\delta_{Fe}<0$ and of sufficient magnitude to ensure

$$K_g < -K_D < 0 \quad (47)$$

and align the spins parallel to c_h. Further,

$$\mu^{Fe} = g_{||}S'\mu_B \approx 4.2\mu_B \quad (48)$$

is a reasonable estimate after account is taken of the additional enhancement of the coefficient a_1 from the molecular-field perturbation $\mathcal{H}_{ex}$.

Crystallographic evidence indicates that $\delta_{Fe}<0$ above T_N. Where the cationic displacements of Eq. (2) are large, the positive contribution to the axial field is reduced and a negative contribution from the shielding anions is enhanced. Therefore large cationic displacements form a negative axial field ($\delta_{Fe}<0$). Figure 2 shows the M^{2+}–Ti^{4+} spacings per rhombohedral-cell length c_R. Since spin-orbit interactions are unimportant for Mn^{2+} and Ni^{2+}, a straight line is drawn between d^5 and d^8. The marked increase in the relative magnitude of the $Fe^{2+}(d^6)$–Ti^{4+} spacings indicates that spin-orbit interactions enhance the displacements, which requires a $\delta_{Fe}<0$. Were $\delta_{Fe}>0$, the Fe^{2+}–Ti^{4+} spacing would be on or below the straight line in Fig. 2.

3. Co^{2+}

In $CoTiO_3$ also, the energy $\mathcal{H}_{ex}$ is optimized below T_N by a $\delta_{Cc}<0$. However, with two β-spin t electrons per Co^{2+} ion, a $\delta_{Co}<0$ corresponds to a positive axial field, or a reduced Co^{2+}–Ti^{4+} separation. From Fig. 2, any such reduction is small. In fact, the separation indicates little influence of preferential ordering of the t hole as a result of $\delta_{Co}\neq 0$, which suggests that $\delta_{Cc}\approx 0$. However, the fact that it was not possible to observe paramagnetic resonance[4] indicates that above T_N, $K_g\neq 0$ and therefore $\delta_{Co}\neq 0$. A negative ($\delta_{Cc}>0$) axial field provides a $K_g>0$ (see the Appendix) which adds to K_D and keeps the spins in the basal planes below T_N. However, with collinear spins below T_N, a cooperative adjustment of the atomic positions (a magnetostriction) would occur so as to optimize the spin-orbit-coupling stabilization, and this striction would reduce δ_{Co} toward $\delta_{Co}=0$, where the energy V_{LS} reaches its full value. Since no further spin-orbit-coupling energy would be gained by a $\delta_{Co}<0$, since the spins are maintained in the basal planes by $K_D>0$, any magnetostriction would leave $\delta_{Co}\geq 0$. Thus for small $\delta_{Co}>0$ above T_N, it is reasonable to expect that below T_N, $\delta_{Co}\approx 0$ and

$$K_g \approx 0. \quad (49)$$

Any positive ($\delta_{Co}<0$) axial field in the paramagnetic phase is improbable [see discussion after Eq. (55)].

Since $\lambda\approx -180$ cm^{-1} and $k_c\approx 0.89$ [5] for octahedral-site Co^{2+} ions in an oxide, the Kramers doublet ground state $J=\frac{1}{2}$ for the case $\delta_{Co}=0$ is separated from the next higher $J=\frac{3}{2}$ state by $9k_c\lambda/4\approx 360$ cm^{-1}. This is much larger than any axial-field splitting of the $J=\frac{3}{2}$ state, and the doublet ground state having $S'=\frac{1}{2}$ remains well separated from it. For $\delta_{Co}=0$ and $\mathcal{H}_{ex}=0$, the coefficients of the ground-state wave function shown in Table I are

$$b_1 = \tfrac{1}{2}\sqrt{2}, \qquad b_2 = -\sqrt{3}, \qquad b_3 = \tfrac{1}{6}\sqrt{6}, \quad (50)$$

and the g factor is isotropic:

$$g_{||} = g_\perp = 3.33 + k_c. \quad (51)$$

Below T_N, the exchange energy introduces a molecular field perpendicular to c_h that decreases b_1, b_3 and increases b_2 to make $g_\perp > 3.33 + k_c$ (see Table I). Given $S'=\frac{1}{2}$ and the magnitude of J_p obtained from Fig. 7, this gives a low-temperature atomic moment

$$\mu^{Co} = (g + \Delta g)\,S'\mu_B \approx 2.5\mu_B. \quad (52)$$

Note that the coefficients b_i are quite sensitive to $\mathcal{H}_{ex}$. This is reflected in the much higher Co^{2+} moment, $\mu^{Co}\approx 3.7\mu_B$, found in CoO.

[4] J. J. Stickler, S. Kern, A. Wold, and G. S. Heller, preceding paper, Phys. Rev. **164**, 765 (1967).
[5] W. Low, Phys. Rev. **109**, 256 (1958).

TABLE IV. Exchange parameters in °K as determined from paramagnetic Curie temperature Θ_p, Néel temperature T_N, magnetic susceptibility at the Néel temperature $\chi_m(T_N)$, antiferromagnetic resonant frequency ω_R, and anisotropy constant $K=K_D$.

Sample \ Datum $2J/k$	Θ_p $2J_p/k$	T_N $2J_N/k$	$J_{++}=\frac{1}{2}(J_p+J_N)$ $2J_{++}/k$	$J_{+-}=\frac{1}{2}(J_p-J_N)$ $2J_{+-}/k$	$\chi_m(T_N)$ $2J_{+-}/k$	ω_R $2J_{+-}/k$
$MnTiO_3$	−75.0	21.8	−26.6	−48.4	−50±5[a]	−22.5[b]
$FeTiO_3$	50.0	31.0	40.5	9.5	•••	•••
$CoTiO_3$	35.0	49.7	42.3	−7.3	•••	−7.2
$NiTiO_3$	−16.4	34.5	9.0	−25.5	−28.3	−34.2

[a] Uncertainty due to anomaly in χ_m versus T just above T_N.
[b] If $\mu^{Mn}=4.55\mu_B$, so that $K_D=-1.3\times10^6$ erg/cm^3, then resonance data give $2J_{+-}/k=-27$°K.

VII. COMPARISONS WITH EXPERIMENT

A. Neutron Diffraction

Neutron-diffraction studies[6–8] have not only provided the refined M^{2+}–Ti^{4+} separations plotted in Fig. 2, but have also determined the magnetic order and provided the values for the experimental atomic moments displayed in Table III. The magnetic order was in each case that predicted by Table II, which indicates that in $MnTiO_3$ the parameter J_3 is sufficiently larger than J_4 and J_4' that

$$J_3+3J_4'>6J_4. \tag{53}$$

This relationship could not be unambiguously predicted from our qualitative considerations of superexchange.

The fact that the spin directions were found to agree with prediction substantiates the two inferences from the data of Fig. 2: that $\delta_{Fe}<0$ and $K_g<-K_D<0$ in $FeTiO_3$, and that $\delta_{Co}\approx0$ and $K_g\approx0$ in $CoTiO_3$.

The only significant discrepancy between theory and experiment is the magnitude of the Mn^{2+} atomic moment. Although it is tempting to blame this discrepancy on an incorrect form factor for Mn^{2+}, this is not a plausible explanation. Not only have neutron-diffraction results consistently shown a reduced moment for magnetically ordered Mn^{2+}, but magnetization measurements have been able to demonstrate directly that this is the case in $Mn[Cr_2]S_4$.[9] Therefore this discrepancy must be assumed to be real.

B. Magnetic Susceptibility and Resonance

Table IV displays values of the exchange parameters obtained from magnetic susceptibility with the aid of Eqs. (22) and (23) for $MnTiO_3$ and $NiTiO_3$, with Figs. 7 and 8 and Eq. (31) for $FeTiO_3$ and $CoTiO_3$. These are compared with parameters obtained from resonance data with the aid of Eq. (25). No magnetic resonance was observed in $FeTiO_3$, which is compatible with the assumption of a large anisotropy ($g_\perp\approx0$).

The susceptibility of $MnTiO_3$ exhibits a broad peak near 100°K rather than a well-defined peak at $T_N=$ 63.5°K, whereas all the other MTiO$_3$ ilmenites exhibit a sharp maximum in χ_m at T_N. Although specific-heat measurements[10] have shown that 45% of the magnetic entropy remains in $MnTiO_3$ when the temperature is raised to T_N, a similar amount of short-range order was also found in $FeTiO_3$. Therefore, short-range order alone cannot be responsible for an anomaly that is associated only with $MnTiO_3$. It may be argued qualitatively that the short-range clusters above T_N are within basal planes, and that in $MnTiO_3$ these would be antiferromagnetic, thus decreasing χ_m, whereas in $FeTiO_3$ they would be ferromagnetic, thus increasing χ_m. The fact[11,12] that the layered compounds K_2NiF_4 and K_2MnF_4, which also have antiferromagnetic coupling within layers like $MnTiO_3$, have a similar broad maximum above T_N in χ_m versus T supports the idea that the anomaly is associated with antiferromagnetism in the layers. However, short-range order alone may not be sufficient to account quantitatively for the phenomenon. This would then be a second discrepancy between theory and experiment for the compound $MnTiO_3$.

A third discrepancy in $MnTiO_3$ is the low value of $2J_{+-}/k$ obtained from resonance data as compared with that for susceptibility data. Even if a $\mu^{Mn}=4.55\mu_B$ were chosen, giving $K_D=-1.3\times10^6$ erg/cm^3, the resulting value −27°K is still too low. One might argue that there are four sublattices and the resonance mode is not the one usually observed. However, since the antiferromagnetic order A_1A_2 antiparallel to B_1B_2 of Fig. 1 does not enlarge the unit cell, only two magnetic sublattices are possible. In order to have a four-sublattice model giving another resonant mode as the low-frequency mode, it would be necessary to have noncollinear spins, and neutron-diffraction data give no evidence of such spin canting. This means that the susceptibility and resonance data can only be recon-

[6] G. Shirane, S. J. Pickart, R. Nathans, and Y. Ishikawa, J. Phys. Chem. Solids **10**, 35 (1959).
[7] G. Shirane, S. J. Pickart, and Y. Ishikawa, J. Phys. Soc. Japan **14**, 1352 (1959).
[8] R. E. Newnham, J. H. Fong, and R. P. Santoro, Acta Cryst. **17**, 240 (1964).
[9] N. Menyuk, K. Dwight, and A. Wold, J. Appl. Phys. Suppl. **36**, 1088 (1965).
[10] D. Smith, thesis, Massachusetts Institute of Technology, 1965 (unpublished).
[11] G. G. Srivastava, Phys. Letters **4**, 55 (1963).
[12] D. J. Breed, Phys. Letters **23**, 181 (1966).

ciled within the framework of molecular-field theory if there is an additional anisotropy energy

$$K_g^{\mathrm{Mn}} \approx -0.5K_D > 0. \tag{54}$$

This third discrepancy cannot be accounted for on the basis of short-range order. The integral of the magnetic specific heat[10] over temperature gives 223.5 cal/mole, which should equal the exchange energy of the ordered spins at 0°K. This gives an independent $2J_N/k = 36$°K and therefore, from Table IV, a corresponding $2J_{+-}/k = -55$°K, which only aggravates the problem. There is a similar, though less pronounced, discrepancy for $NiTiO_3$, where the additional anisotropy energy required is

$$K_g^{\mathrm{Ni}} \approx 0.2K_D > 0. \tag{55}$$

The data for $CoTiO_3$ show surprising consistency, considering the complicated calculations for J_p and J_N. The anticipation of a $\delta_{\mathrm{Co}} \approx 0$ in order to optimize the energy V_{LS} for basal-plane spins is consistent with the data. The fact that Co^{2+} in Al_2O_3:Co has a $k_g > 0$,[13] corresponding to a negative trigonal field ($\delta_{\mathrm{Co}} > 0$), does not negate this conclusion, since the isolated Co^{2+} ions are not magnetically ordered and cannot induce a static magnetostriction. Further, the effective charge on a Ti^{4+} ion should be larger than that on an Al^{3+} ion, thus favoring the positive component of the axial field.

Finally, the fact that $J_N < J_p$ for $FeTiO_3$ in Table IV is not surprising in view of the fact that the theory for J_p and J_N is not applicable where $\delta_{\mathrm{Fe}} < 0$. It is only further evidence that $FeTiO_3$ has an anomolously large Fe^{2+}–Ti^{4+} separation because it optimizes the energy V_{LS}. The compound $FeTiO_3$ probably has an extremely small $g_\perp$.

VIII. DISCUSSION

A. A New Correlated Superexchange

This analysis clearly shows that present theory is inadequate to account for the magnetic properties of $MnTiO_3$. Since the theory gives good agreement with resonance experiments for isolated Mn^{2+} ions in a nonmagnetic host[14] and since a reduced manganese atomic moment appears to be a general property of magnetically coupled Mn^{2+} ions, we may conclude that the discrepancy is due to a many-body, superexchange interaction not adequately accounted for in the perturbation $\mathcal{H}_{\mathrm{ex}}$. In the conventional theory for $\mathcal{H}_{\mathrm{ex}}$, there are two principal superexchange contributions: These have been referred to as delocalization superexchange and correlation superexchange.[3] In the former, the excited state that mixes with the crystal-field ground state consists of an electron transfer from one cation to its near neighbor; and in the latter, it consists of a simultaneous transfer of two electrons from an intermediary anion, one to each of the interacting cations. In both cases transfer of an electron is accomplished only at the cost of considerable electrostatic energy, since the ions contain different numbers of electrons. This fact suggests that a competitive coupling mechanism would be via an excited state that kept the number of electrons per ion the same. Such a mechanism can be readily formulated: It consists of a correlated delocalization superexchange in which the two interacting ions each transfer and receive an electron simultaneously. This corresponds to the simultaneous transfer of an electron-hole pair. Therefore it will be referred to as *exciton superexchange*. Such a correlated superexchange would be proportional to the square of an exciton transfer integral, similar to the one-electron transfer integrals of the other two superexchange contributions, and inversely proportional to the excitation energy, which in this case would be the sum of the two ionic excited states. This energy is known fairly accurately from crystal-field theory and optical measurements of the term splittings. Where this mechanism can occur, the sign of the coupling is the same as for the individual delocalization superexchange contributions that are occurring simultaneously, so that this contribution is additive. Further, where the ionic excited states are close to the ground state, this new correlated superexchange can be the most important contribution.

To illustrate the mechanism, consider the coupling J_1 between the Mn^{2+} ions within the basal planes of $MnTiO_3$. As illustrated in Fig. 9, both cation-cation and 90° cation-anion-cation interactions contribute to J_1. Each of the d orbitals of the ground-state Mn^{2+} ions is half-filled, so that the net interaction is antiferromagnetic. Therefore, transfer of an exciton creates a spin-forbidden excited state. Optical measurements[15–17] on compounds containing isolated Mn^{2+} ions versus those containing Mn^{2+} ions sharing common octahedral-site edges, as in $MnTiO_3$, have shown an enhancement (as much as tenfold) of the spin-forbidden, parity-forbidden absorption bands to $^4A_{1g}$, ^4E_g, and other excited states where the manganese ions are coupled. This appears to be direct evidence of the exciton superexchange mechanism.

The cation-cation interactions involve a simple interchange of t electrons, which mixes in an excited state only if the ions are coupled antiparallel. The 90° cation-anion-cation interactions couple an e and a t orbital, and the transferred exciton originates as an e electron and a t hole to make the $S = \frac{3}{2}$ excited state on each cation t^4e^1. This has lower energy than either the $^4A_{1g}$ excited state of the cation-cation interaction or the t^2e^3 excited state, since the crystalline fields stabilize

[13] W. Low and E. L. Offenbacher, in *Solid State Physics*, edited by F. Seitz and D. Turnbull (Academic Press Inc., New York, 1965), Vol. 17, p. 204.
[14] W. Low, Phys. Rev. **105**, 793 (1957).
[15] D. S. McClure, J. Chem. Phys. **39**, 2850 (1963).
[16] J. Ferguson, H. J. Guggenheim, and U. Tanabe, J. Phys. Soc. Japan **21**, 692 (1966).
[17] L. L. Lohr, Jr., Bull. Am. Phys. Soc. **11**, 243 (1966).

the t orbitals relative to the e orbitals. In fact, this excited state may have an energy quite close to the ground state, since these are separated only by the difference between the Hund intra-atomic-exchange splitting and the crystal-field splitting of e and t orbitals, which are of comparable magnitude. Not only so, but the $S=\frac{1}{2}$ low-spin-state t^5e^0 is expected to be of even lower energy, so that the dominant mechanism should be a double-exciton superexchange. (A low-spin ground state is known, but not an intermediate-spin ground state.) Therefore, exciton superexchange mixes the $^2T_2(t^5e^0)$ and the two $^4T_{1g}(t^4e^1)$, $^4T_{2g}(t^4e^1)$ excited states into the $^6A_{1g}(t^3e^2)$ ground state. In addition, the energies of these excited states are probably much closer to the ground state than are any polar excited states required for conventional superexchange mechanisms, so that it could be the dominant superexchange mechanism in the J_1 of $MnTiO_3$.

B. Consequences of Exciton Superexchange

A significant feature of this mechanism is that in the paramagnetic state, where the near-neighbor spins are not aligned, exciton transfer is minimized. This suggests that as for the isolated Mn^{2+} ion, so for the magnetically disordered Mn^{2+} ion, the effective g and S values are 2 and $\frac{5}{2}$, as predicted in Table I. Therefore, high-temperature susceptibilities should give an effective atomic moment

$$\mu_\infty{}^*=g[S(S+1)]^{1/2}\mu_B=5.91\mu_B, \qquad (56)$$

which is what is found experimentally.[4] However, throughout the region of short-range magnetic order, there must then be an increase with decreasing temperature in exciton transfer and therefore an increased mixing of excited quartet and/or doublet states into the ground state. Therefore just above the Néel temperature, it is possible to have a change in the magnitude of the atomic moment from the high-temperature value of Eq. (56) to the low-temperature value for the magnetically ordered state. Given the neutron-diffraction value $4.55\mu_B=g'S'\mu_B$ at low temperatures, it is reasonable to expect that at the Néel temperature the effective paramagnetic moment corresponds to

$$\mu_N{}^*\approx 5.5\mu_B. \qquad (57)$$

It follows that in the interval of short-range order just above T_N, the temperature dependence of the susceptibility would become modified;

$$d\chi_m/dT=\chi_m\{-(T-\theta)^{-1}+[2(1+\Lambda\chi_m)/\mu^*]d\mu^*/dT+\chi_m d\Lambda/dT\}, \qquad (58)$$

where $\Lambda=\frac{1}{2}(\Lambda_{++}+\Lambda_{+-})$. For an exponential increase in μ^* above T_N,

$$\mu^*=\mu_\infty{}^*\exp[-\ln(\mu_\infty{}^*/\mu_N{}^*)\times(T_N-\tau)/(T-\tau)], \qquad (59)$$

where τ is an adjustable parameter and $\ln(\mu_\infty{}^*/\mu_N{}^*)\approx 0.07$ is introduced as a convenient phenomenological parameter. In this model, $d\Lambda/dT>0$ and $\Lambda\chi_m>-1$. Thus it is possible to choose a $d\Lambda/dT$ and a τ to account for the anomalous broad maximum in χ_m versus T some 35°K above T_N. To what extent such a mechanism contributes to the anomaly is not clear. Short-range order plus antiferromagnetic order within the planes probably makes an important contribution, if not the most important contribution.

Another important consequence of exciton transfer is that the excited $^4T_{1g}$, $^4T_{2g}$, and $^2T_{2g}$ states all carry an angular momentum and may therefore contribute to the anisotropy energy K_g in the presence of a $V_T\neq 0$. The combined perturbation $(V_{LS}+V_T)$ splits the ^4T states as shown in Fig. 5 for the $^4T_{1g}$ states of Co^{2+}, and the lowest level is a doublet having $S'=\frac{1}{2}$, which is itself split by the molecular-field energy $\mathcal{H}_{ex}$. Thus the wave function of lowest energy is

$$\Phi_4=c_1\,|\,-1,\tfrac{3}{2}\rangle+c_2\,|\,0,\tfrac{1}{2}\rangle+c_3\,|\,1,-\tfrac{1}{2}\rangle. \qquad (60)$$

With one β-spin t electron, a negative axial field favors $g_{\|}>g_\perp$, corresponding to $K_g<0$, and a positive field favors $g_{\|}<g_\perp$, corresponding to $K_g>0$. The $^2T_{2g}$ state also has a doublet lowest level;

$$\Phi_2=d_1\,|\,1,-\tfrac{1}{2}\rangle+d_2\,|\,0,\tfrac{1}{2}\rangle. \qquad (61)$$

However, with two β-spin t electrons, a negative axial field favors $g_{\|}<g_\perp$, corresponding to $K_g>0$, and a positive axial field favors $g_{\|}>g_\perp$, corresponding to $K_g<0$. Now reconciliation of magnetic susceptibility and resonance data requires, according to Eq. (54), a $K_g{}^{Mn}>0$. Thus the exciton-transfer mechanism can also account for this third discrepancy provided that

$$E(^4T)<E(^2T) \quad \text{and} \quad V_T>0 \qquad (62)$$

or

$$E(^4T)>E(^2T) \quad \text{and} \quad V_T<0. \qquad (63)$$

From the magnitude of the Mn^{2+}–Ti^{4+} separation shown

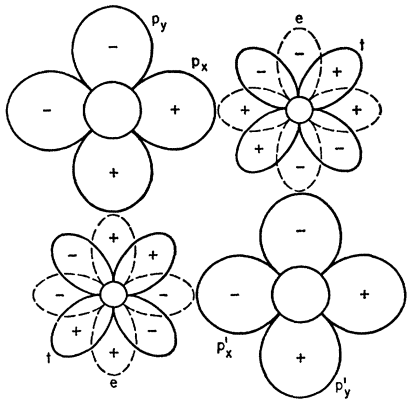

FIG. 9. Anionic p and cationic t and e orbitals active in superexchange between two octahedral-site cations sharing a common octahedral edge. The t orbitals overlap directly (cation-cation superexchange) and a t on one cation overlaps an e on the other via an anionic p orbital that π-bonds with the first and σ-bonds with the second (90° cation-anion-cation superexchange).

in Fig. 2, it is concluded that $V_T<0$ and therefore that Eq. (63) is the dominant alternative. An $E(^2T)<E(^4T)$ is consistent with the fact that stable low-spin ions are known, whereas no stable ions of intermediate spin are known. (The expression for double-exciton superexchange is similar to that for simple exciton superexchange provided that a two-exciton transfer integral is used.)

Exciton superexchange is a general mechanism and therefore should manifest itself with other ions. However, in order to get a reduction in the ionic moments, the coupling must be antiferromagnetic. Further, an abnormal reduction in the atomic moment requires a double-exciton superexchange. This requires overlap of half-filled t and e orbitals, as in the 90° cation-anion-cation interactions discussed above for $MnTiO_3$. This situation can only occur in $^6S(t^3e^2)$ ions like Mn^{2+} and Fe^{3+}. In the case of Fe^{3+} ions, there are not many compounds in which Fe^{3+} ions share common octahedral-site edges and are coupled antiferromagnetically. However, there are antiferromagnetic compounds with ~130° cation-anion-cation interactions. It would be of interest to study systematically the magnitudes of the low-temperature atomic moments in these compounds.

In the case of $NiTiO_3$, the exciton transferred originates as a t electron and an e hole. Since the t orbitals are filled in the $^3A_{2g}$ state, the transferred-electron spin is antiparallel to the net spin, so that the coupling is ferromagnetic and the excited states are $^3T_{1g}(t^5e^3)$ and $^3T_{2g}(t^5e^3)$. Thus there is no change in atomic moment, which is consistent with observation. In addition, there is no term of competitive energy corresponding to a double-exciton transfer, so that there are only one-exciton excited states contributing to K_g. The lowest excited state is a singlet ($J=0$), but the other two multiplets ($J=1$ and 2) do contribute an anisotropic energy in the presence of a trigonal crystalline field. With one t hole in the excited state, it follows that

$$K_g^{\mathrm{Ni}}>0 \quad \text{if} \quad V_T<0, \tag{64}$$

$$K_g^{\mathrm{Ni}}<0 \quad \text{if} \quad V_T>0. \tag{65}$$

The fact that a $K_g^{\mathrm{Ni}}>0$ is required to reconcile resonance and susceptibility data is consistent with a small, negative trigonal field in $NiTiO_3$.

It is concluded that the magnetic data on the ilmenites $MTiO_3$ can be satisfactorily interpreted by crystal-field, molecular-field, and superexchange theories provided that a new contribution to cation-anion-cation superexchange is introduced. This contribution involves an exciton transfer that mixes excited ionic states into the ground state. With antiferromagnetic coupling, these are spin-forbidden excited states. For the ^6S ions Mn^{2+} and Fe^{3+}, a double-exciton transfer may dominate the 90° cation-anion-cation superexchange. In this case the excited states are of much lower net spin, and there is a noticeable reduction in the atomic moment in the magnetically ordered state. Finally, in the presence of noncubic fields these excited states may contribute an anisotropy energy. This is essentially a many-atom anisotropy term, since the excited states are induced by superexchange coupling.

ACKNOWLEDGMENT

We are happy to express our gratitude to Herbert J. Zeiger for several helpful discussions during the progress of this work.

APPENDIX

In order to derive an analytic expression for K_g in the case of octahedral-site Co^{2+}, it is customary[18] to note that there is an anisotropy that enters the many-atom superexchange energy as a result of the relationship between the true spin $S=\frac{3}{2}$ and the effective spin $S'=\frac{1}{2}$. Within the ground state of Table I, the matrix elements of S_x, S_y, and S_z have the form of the spin-$\frac{1}{2}$ Pauli spin matrices multiplied by q, q, and p, respectively, where

$$q=b_2^2+\sqrt{3}b_1b_3 \quad \text{and} \quad 2p=3b_1^2+b_2^2-b_3^2. \tag{A1}$$

Therefore, it is possible, in the many-atom superexchange operator $\mathcal{H}_{\mathrm{ex}}$, to formally replace the true spin-$\frac{3}{2}$ operator $\mathbf{S}$ by the effective spin-$\frac{1}{2}$ operator $\mathbf{S}'$, where

$$S_x=2qS_x', \qquad S_y=2qS_y', \qquad S_z=2pS_z'. \tag{A2}$$

Thus the superexchange operator becomes

$$\mathcal{H}_{\mathrm{ex}}=-\sum_{ij}\left(J_{ij}'\mathbf{S}_i'\cdot\mathbf{S}_i'-D_{ij}S_{iz}'S_{jz}'\right), \tag{A3}$$

where

$$J_{ij}'=4q^2J_{ij} \quad \text{and} \quad D_{ij}=(4q^2-4p^2)J_{ij}. \tag{A4}$$

This gives an anisotropy energy

$$K_g=\tfrac{1}{2}NS^2[(q^2-p^2)/p^2]J_p \tag{A5}$$

having $q<p$ for positive axial fields ($\delta_{\mathrm{Co}}<0$) and $q>p$ for negative ($\delta_{\mathrm{Co}}>0$) axial fields.

[18] M. E. Lines, Phys. Rev. **131**, 546 (1963).